A PRELIMINARY COMPARISON OF BEAM INSTABILITIES AMONG ESRF, APS, AND SPRING-8 X-RAY STORAGE RING LIGHT SOURCES*

K. Harkay, APS/ANL, Argonne, USA; R. Nagaoka, J.-L. Revol, ESRF, Grenoble, France;
T. Nakamura, JASRI/SPring-8, Hyogo, Japan†

1 INTRODUCTION

The development of high-brilliance, hard x-ray synchrotron radiation sources enables a broad range of basic and applied research at the forefront in fields such as materials science; biological science; physics; chemistry; environ-mental, geophysical, and planetary science; and innovative x-ray instrumentation. The three highest energy, highest brightness light sources are ESRF, APS, and SPring-8. Maintaining high performance in these sources is a primary goal, as is understanding limitations due to the coupling impedance and beam instabilities. A series of studies, both experimental and theoretical, have been carried out independently at each facility. The similarity of the machines and user requirements provided the motivation to compare the characteristics of the three rings.

1.1 Machine parameters

The ESRF, APS, and SPring-8 storage rings, commissioned within a few years of each other, are generally similar in their main parameters (Table 1). Nevertheless, different design choices were made, especially concerning the vacuum chambers that accommodate the IDs (Table 2). At APS, all the straight sections dedicated to x-ray production are equipped with small-gap vacuum chambers. In contrast, at SPring-8, mostly in-vacuum IDs are used, while at ESRF mostly in-air IDs are used with chambers of different gaps and materials.

1.2 Impedance budget

Table 1: Representative parameters for the three rings.

	ESRF	APS	SPring-8
Energy [GeV]	6.0	7.0	8.0
Circumference [m]	844.4	1104	1436
RF frequency [MHz]	352.2	351.9	508.6
RF harmonic no.	992	1296	2436
Nominal RF voltage [MV]	9.0	9.5	16
Momentum compaction	1.86×10^{-4}	2.9×10^{-4}	1.46×10^{-4}
Synchrotron tune	6.0×10^{-3}	7.0×10^{-3}	1.0×10^{-2}
Emittance H [nm·rad]	3.7	3.9	6.0
Coupling [%]	0.5 %	1 %	0.2 %
Nom. chromaticity, ξ[1] H/V	5.46/5.75	5/7	7/6
Damping time H/V/L [ms]	7/7/3.5	9.5/9.5/4.7	8.3/8.3/4.2

[1] $\xi = \Delta Q/(\Delta p/p)$; for ESRF: nominal multibunch mode (single bunch: 7.6/12.9)

The primary contributions to the coupling impedance include the geometry, conductivity, and number of small-gap ID chambers. The influence of the RF cavity higher order modes (HOMs) depends in part on the β–function at the cavities. Also, the average β, the optics, and impedance of the tapers between the regular and ID chambers must be considered [1]. For the in-vacuum IDs, a thin conductive sheet on the NdFeB magnet serves to reduce the resistive wall (RW) impedance. At SPring-8, thin Cu 10 μm + Ni 50 μm sheets are used to give a reduction factor of 0.75, relative to unshielded magnets. For the long (30 m) straight sections, Cu 50 μm + Ni 10 μm sheets give a reduction factor of ~ 0.25 [2].

Table 2: Representative parameters for the impedance.

	ESRF	APS	SPring-8
No. of straight sections	32	40	44+4 long
No. of in-vacuum IDs	4 (2 m)	0	13+1 long
No. of small-gap chambers*	28	25	3
Vacuum chamber material	SS/Al/Cu	Al	Al
No. of flanges	571	480	700
No. of bellows/RF fingers	290	160	600+28[2]
No. of BPMs	224	360	266
No. of RF cavities (No. cells)	6*(5)	16*(1)	32*(1)

[2] for in-vacuum IDs

* At SPring-8: gap=15 mm, matl=SS; details for ESRF and APS:[3]

ESRF			APS		
No.	Gap	Matl	No.	Gap	Matl
16	11.0	SS	22	8.0	Al
2	11.0	Al	2	5.0	Al
4	8.0	Cu	1	19.6	Al
1	8.0	SS			
5	15.0	SS			

[3] No: Number of elements. Gap: Minimum internal aperture in mm. Matl: Chamber material (Cu = copper-coated)

1.3 Bunch filling patterns

A typical operating requirement is high average brilliance. At ESRF, 200 mA uniform filling is commonly delivered with a beam lifetime close to 80 h. At APS, growing user demand for time-resolved experiments has led to a decision to operate in a few-bunch mode most of the time. Top-up mode [3] used with a low-horizontal-emittance lattice overcomes the limitations of the shorter lifetime (< 10 h).

Table 3: Filling patterns delivered and % of total user beam time

	ESRF			APS			SPring-8		
	Mode	mA	%	Mode	mA	%	Mode	mA	%
Multibunch									
Uniform	992 BT	200	30				(12-1)× 116 BT[5]	100	45
Partial	2/3; 2*1/3	200	35						
Few Bunch									
Single		20	8						
Multiple	16*1	90	22	23*1 TU[4]	100	71	203	100	12
				23*1	100	15	84×4 BT	100	6
							29×11 BT	100	12
Hybrid	1/3+1	200	5	1/8+3	100	7	1/2+18	100	19
				1/8+1	100	7	10/84+73	100	6

[4] TU = top-up mode: 3.9 nm-rad lattice; non-TU: 7.5 nm-rad lattice.

[5] No. of trains × (bunches in train)BT

*Work at ANL supported by U.S. Department of Energy, Office of Basic Energy Sciences under Contract Nos. W-31-109-ENG-38.

† harkay@aps.anl.gov, ryutaro.nagaoka@soleil.u-psud.fr, revoljl@esrf.fr, nakamura@spring8.or.jp

2 SINGLE BUNCH ISSUES

2.1 Bunch length and energy spread

The bunch length (σ_t) is measured using a dual-sweep streak camera. The relative energy spread (σ_δ) is computed by measuring the transverse beam size either from a single, dispersive source (SPring-8), or from two sources, one dispersive and one nondispersive (ESRF, APS). At low intensity in all three rings, the bunch length grows in the potential well regime (σ_δ remains constant) (Fig. 1). Above a threshold intensity, the energy spread grows in the microwave regime. The thresholds are 10, 18, and 23 nC for ESRF, APS, and SPring-8, respectively.

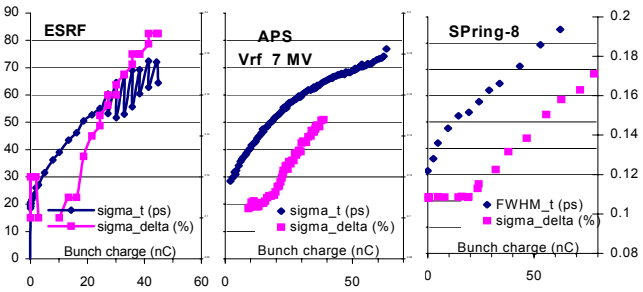

Figure 1: Bunch length and energy spread (APS: [4,5])

2.2 Mode merging at zero (or low) chromaticity

The transverse mode-coupling instability (TMCI) between modes 0 and –1 sets a severe intensity limitation for $\xi \approx 0$. Adding small-gap ID chambers incrementally lowers the intensity threshold. The measured intensity thresholds are summarized below. The measured tune depression and mode crossing at ESRF are shown in Fig. 2.

Intensity threshold (I_{th}):

ESRF:	I_{th} [H]: 5.6 nC (2 mA)	I_{th} [V]: 2.3 nC (0.8 mA)
APS:	I_{th} [H]: 15 nC (4 mA)	I_{th} [V]: 7.4 nC (2 mA)
SPring-8:	I_{th} [H]: 24 nC (5 mA)	I_{th} [V]: 19 nC (4 mA)

At all three rings, modeling using a broad-band (BB) resonator impedance reproduces the TMCI threshold for $\xi = 0$. The modeling parameters are summarized below. At SPring-8, simulations using wake functions based on MAFIA calculations predict a dependence of the head-tail instability and TMCI thresholds on chromaticity that show good agreement with experiments [7]. Recently, raw wake functions were used to simulate the longitudinal motion, and better agreement was obtained for high bunch intensity. A similar analysis is planned at APS.

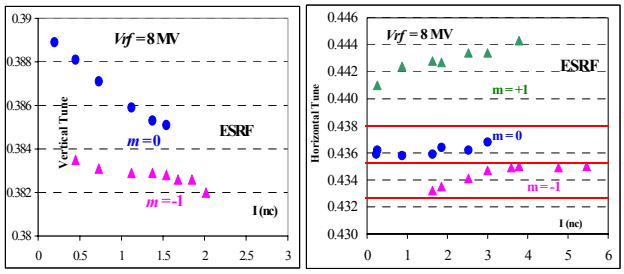

Figure 2: Measured detuning of head-tail mode 0 and –1, vertical (left) and horizontal (right), example from ESRF (see Ref. [6] for APS and Ref. [7] for SPring-8).

Longitudinal broad-band impedance model:

ESRF:	f_{res} = 30 GHz	R_s = 42 kΩ	Q=1
APS:		Z/n=0.5 Ω	Q=1 [4]

Vertical broad-band impedance model:

ESRF:	f_{res} = 22 GHz	R_s = 6.5 MΩ/m	Q=1
APS:	f_{res} = 25 GHz	R_s = 1.2 MΩ/m	Q=1 [6]

2.3 High chromaticity regime

At all three rings, a positive chromaticity avoids the TMCI and raises the intensity threshold nonlinearly in both planes. In addition, the bunch lengthening with intensity helps stabilize the higher order head-tail modes. The single-bunch intensity limits are:

ESRF:	56 nC (20 mA)	ξ_h=9.1	ξ_v=13
APS:	33 nC (9 mA)[6]	ξ_h=5	ξ_v=6
SPring-8:	77 nC (16 mA)[7]	ξ_h=7	ξ_v=6

[6] for 3.9 nm-rad lattice, not optimized

[7] with in-vacuum ID gaps open; 7 nC (1.5 mA) for user mode

At ESRF, in the horizontal plane, the instability evolves in the head-tail regime. In the vertical plane, the incoherent frequency spread induced by longitudinal instabilities is large enough to entirely stabilize the head-tail regime. To reproduce the observed threshold, a post head-tail (PHT) mechanism is invoked for $\xi > 0.2$. The PHT regime is stabilized by the σ_δ, which induces an incoherent spread of the betatron frequency [8,9]. The instability rise time then becomes shorter than the synchrotron period, and the notion of modes is invalidated.

At APS, the intensity limit is lower than that predicted by the PHT regime. Injection transients couple horizontal to vertical motion, and the beam is lost on the 5-mm min. vertical aperture. Also, a large horizontal oscillation is typically observed above the TMCI threshold but below the intensity limit; this sets the operational limit [5]. Increased sextupole strength or feedback may be required.

At SPring-8, no coherent bunch motion is observed in either plane for $\xi > 4$, and the single bunch intensity is limited by outgassing caused by parasitic losses.

2.4 Test or plan for feedback

Feedback is a key issue for high-single-bunch intensity in order to reduce the required chromaticity, since high ξ reduces the lifetime. Tests performed at ESRF increased the TMCI threshold by five but were not successful at higher ξ values. A transverse bunch-by-bunch feedback is planned at APS to increase the effective single bunch limit and for use in bunch cleaning.

3 MULTIBUNCH ISSUES

3.1 Longitudinal coupled bunch instability (CBI)

Precise temperature control of the RF cavities readily avoids a strong HOM-driven longitudinal CBI observed at ESRF. Extra stabilization is obtained using partial filling patterns, which produces Landau damping from the

bunch-to-bunch synchrotron frequency spread. The case is similar at APS, where longitudinal CBIs were observed and cured by the temperature control in early operation with long bunch trains. In addition, the RF cavity lengths vary, staggering the HOM resonant frequencies. In anticipation of higher current operation, HOM damper prototypes have been built, and installation is planned. Longitudinal CBIs have not been observed at SPring-8.

3.2 Transverse coupled bunch instability

At SPring-8, transverse HOM-driven CBIs are observed below 70 mA in the horizontal plane with low ξ_h; they are cured with $\xi_h = 7$ (at the cavities, $\beta_h = 25$ m) [10]. Transverse CBIs have never been seen at ESRF (the average β is much lower). Transverse CBIs are possibly seen at APS, but the threshold occurs for a smaller ξ than that needed for single bunch; it is therefore not an operational limitation.

3.3 Transverse resistive wall instability

At ESRF, multibunch operation is strongly affected by transverse RW instabilities. The effect has grown cumulatively with increasing numbers of small-gap ID vacuum chambers. The on-going replacement of SS ID chambers with Al or Cu-coated chambers has had a positive impact. Installation of four in-vacuum IDs (2 m long, 6-mm min. gap) has had no significant impact. With the increased positive ξ, the stabilizing effect of the BB impedance is enhanced [8]. For the vertical plane, simulation of the intensity threshold, including both BB resonator and RW impedances, is in good agreement with the experiment. A strong stabilizing effect of the filling pattern has been observed, as expected from the betatron frequency spread induced by the incoherent betatron tune shift due to the asymmetry of the vacuum chamber cross section [11].

Transverse RW instabilities have only been seen at APS for $\xi_h < 1$ and $\xi_v < 3$. The high conductivity of Al is likely responsible for the relatively high threshold.

These instabilities are now strong at SPring-8 due to the increased number of in-vacuum IDs but are cured by increased chromaticity [2,10].

3.3 Beam-ion instability

At ESRF, horizontal and vertical trapped beam-ion instabilities have been observed during machine time in uniform and partial filling by turning off the ion pumps. At restart, a fast beam-ion instability (FBII) was observed along a uniform bunch train with a 10% gap [8]. The vertical emittance can be significantly degraded in the uniform mode if user delivery is scheduled just after a restart.

No beam-ion instabilities have been observed in preliminary studies at APS at the nominal vacuum pressure of 0.5 nTorr (100 mA). The vacuum could not be degraded by turning off all the ion pumps since the NEG in the antechambers remain activated. There is evidence, however, of electron cloud amplification at specific bunch spacings, leading possibly to electron-stimulated gas desorption and vacuum degradation. These effects will be investigated in future studies [12].

A FBII was observed at Spring-8 after the installation of new chambers in the four long straight sections. It was cured by filling a pattern of shorter bunch trains with 100 ns gaps ((12-1)×116 BT), and ceased after six months of operation as the vacuum pressure improved [13].

3.4 Plan for feedback

At ESRF, a mode-by-mode feedback acting on the first five coupled-bunch modes driven by the vertical RW impedance has been successfully tested in uniform and in 2*1/3 filling, allowing 200 mA operation with $\xi \approx 0$. No deterioration of the beam quality due to the feedback or from transverse HOMs has been observed. Nevertheless, the long lifetime makes the feedback useless for operation. Bunch-by-bunch feedback is planned at SPring-8.

4 DISCUSSION

A very preliminary comparison of the three highest energy storage ring light sources was presented. At APS, a transverse single-bunch instability is most important, while at SPring-8, a multibunch transverse RW instability is dominant. Depending on the operation mode, ESRF faces either single-bunch or transverse RW instabilities. The longitudinal instability characteristics of the rings are similar. Detailed comparisons are planned in the areas of longitudinal impedance and microwave instabilities, and transverse impedance modeling. Of interest is to study the impact of impedance and instability threshold evolution at the three rings and to identify cures to maintain stable operation and undertake high-current development.

5 ACKNOWLEDGMENT

The authors would like to thank all the participants from ESRF, APS, and SPring-8 in these studies.

6 REFERENCES

[1] T.F. Günzel, "Evaluation of the Vertical Transverse Impedance of the ESRF Machine by Element-Wise Wakefield Calculation," these proc.
[2] T. Nakamura et al., Proc. of 2001 Part. Accel. Conf., 1969 (2001).
[3] L. Emery, Proc. of 2001 Part. Accel. Conf., 2599 (2001).
[4] Y.-C. Chae et al., Proc. of 2001 Part. Accel. Conf., 1817 (2001).
[5] K. Harkay et al., Proc. of 2001 Part. Accel. Conf., 1915 (2001).
[6] K.C. Harkay et al., Proc. of 1999 Part. Accel. Conf., 1644 (1999).
[7] Refs. listed in http://acc-web.spring8.or.jp/~nakamura
[8] J.-L. Revol et al., Proc. of 2001 Part. Accel. Conf., 1930 (2001).
[9] P. Kernel et al., Proc of 2000 EPAC, 1133 (2001).
[10] T. Nakamura et al., Proc. of 2001 Part. Accel. Conf., 1972 (2001).
[11] R. Nagaoka et al., Proc. of 2001 Part. Accel. Conf., 3531 (2001).
[12] K.C. Harkay et al., CERN Report No. 2002-001 (Apr. 2002).
[13] T. Nakamura et al., Proc. of 2001 Part. Accel. Conf., 1966 (2001).